



HAL
open science

Two Approaches to Optimal Design of Composite Flywheel

Krzysztof Dems, Jan Turant

► **To cite this version:**

Krzysztof Dems, Jan Turant. Two Approaches to Optimal Design of Composite Flywheel. Engineering Optimization, 2009, 41 (04), pp.351-363. 10.1080/03052150802506521 . hal-00545361

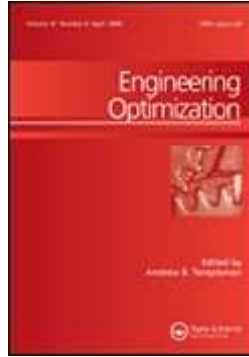
HAL Id: hal-00545361

<https://hal.science/hal-00545361>

Submitted on 10 Dec 2010

HAL is a multi-disciplinary open access archive for the deposit and dissemination of scientific research documents, whether they are published or not. The documents may come from teaching and research institutions in France or abroad, or from public or private research centers.

L'archive ouverte pluridisciplinaire **HAL**, est destinée au dépôt et à la diffusion de documents scientifiques de niveau recherche, publiés ou non, émanant des établissements d'enseignement et de recherche français ou étrangers, des laboratoires publics ou privés.



Two Approaches to Optimal Design of Composite Flywheel

Journal:	<i>Engineering Optimization</i>
Manuscript ID:	GENO-2008-0096.R1
Manuscript Type:	Original Article
Date Submitted by the Author:	05-Sep-2008
Complete List of Authors:	Dems, Krzysztof; Lodz Technical University, Department of Technucal Mechanics and Informatics - K411 Turant, Jan; Lodz Technical University, Department of Technucal Mechanics and Informatics - K411
Keywords:	optimal design, composites, flywheels



Two Approaches to the Optimal Design of Composite Flywheels

Krzysztof Dems* and Jan Turant

Department of Technical Mechanics and Informatics, Technical University of Lodz, Lodz, Poland

In this article two approaches to the design of reinforced composite flywheels are presented. The main goal of the optimization procedure is to maximize the accumulated kinetic energy of a flywheel. The first approach is based on a discrete model of reinforcement, causing the discontinuity of static fields along reinforcement and preserving the continuity of kinematic fields. In the second approach, the material of the reinforced flywheel is subjected to the homogenization procedure using the Halpin-Tsai assumption and then the continuity of both static and kinematic fields is preserved within flywheel domain. The evolutionary algorithm was used in both cases to determine the optimal shape of reinforcements, while the finite element method was applied in order to analyze the mechanical response of a flywheel.

Keywords: optimal design; composites; flywheels

1. Introduction

Flywheels are used in many devices when storing energy is needed. This type of the storage of energy has very important features making flywheels widely used. Flywheel kinetic energy is characterized by high cyclic lifetime, longtime reliability and its high level. These features are currently used in some vehicles for gathering energy lost during deceleration and in low earth orbit satellites which are unable to use their solar batteries while moving in the shadow of the earth. They can be also used in pulsed power supplies for electromagnetic guns or in **UPS (Uninterruptible Power Supply)** devices.

Due to their applicability there are many procedures for solving this seemingly simple problem. Some designers concentrate their effort on proper redistribution of material properties and mass (Eby *et al.* 1999, Kaftanoglu *et al.* 1989, Ries and Kirk 1992) and others design a variety of stack-ply composite structures (Curtiss *et al.* 1995, Thielman and Fabien 2000) to obtain flywheel with maximal energy density. All these approaches have one common feature: each of the designed flywheels is made from durable light material, which is a natural consequence of the linear dependence of energy density with respect to mass density and quadratic dependence on angular velocity.

In this article, the design of fiber-reinforced flywheels of uniform thickness subjected to constant angular velocity is considered. The analysis of the case of the flywheel rotating with variable angular velocity will follow similar steps and is not considered here.

Two different approaches to composite flywheel analysis are presented in the discussed design process. The first approach is based on the concept of reinforcing the structure with a relatively small number of discrete ribs or fibers (cf. Figure 1a). In this case, the reinforcements introduced into the flywheel domain cause the stress discontinuity and preserve continuity of displacement along the middle line of reinforcement (Dems and Mróz 1992, Turant and Dems 2001). The other approach assumes the continuous arrangement of a great number of reinforcements (cf. Figure 1b), which leads to the concept of material homogenization during the analysis process (Jones 1998). In this model, the flywheel is treated as macroscopically uniform with its

* Email: krzysztof.dems@p.lodz.pl

material properties depending on material properties of fiber and matrix. Thus, two different models have to be considered for the purpose of disk analysis, taking into account the fundamental differences in the two above-mentioned approaches. It is assumed that the reinforcements introduced into the disk domain and disk itself are of the same thickness. Thus, the reinforcements constitute the integral part of the flywheel. The problem of delamination of the two phases within the flywheel domain is not considered in this article. Furthermore, the mass fraction and properties of material of reinforcements are the same in both approaches, and the materials of reinforcement and flywheel matrix are assumed to be elastically linear and isotropic. The shape of reinforcing fibers or ribs is described using smooth Bezier curves.

The energy accumulated in the flywheel depends on angular velocity, which also in an obvious manner influences stress intensity. The stress distribution in fiber or rib reinforcing the wheel is a function of the orientation of the middle line of strengthening elements, and hence it can change during modification of the reinforcement line shape. In the present article, the main goal of the designing process is to determine the shape of the reinforcing line so as to obtain the maximum strength flywheel. Such assumption leads to the design of the flywheel which can be subjected to maximal admissible angular velocity and consequently can store the maximal kinematic energy. Both approaches, i.e. discretely and continuously distributed reinforcements, are discussed and the results of design procedure are compared.

2. Problem formulation for flywheel with discrete rib-reinforcement

The composite flywheel of uniform thickness (cf. Figure 2), rotating with constant angular velocity ω and then loaded by distributed centrifugal force equal to $\mu r \omega^2$, is considered. μ denotes here an average matrix and fiber mass density and r determines the radial coordinate of a chosen material point. The flywheel has free external boundary S_e and it is supported on the internal boundary S_i so that the tangential displacements are equal to zero.

$$u_t = 0 \quad \text{along } S_i \quad (1)$$

The flywheel is composed from the uniform disk reinforced with some fibers or ribs introduced in its domain, whose number is relatively small. The volume of reinforcements is assumed to be constant but the shape of their middle lines can undergo changes ($\Gamma \rightarrow \Gamma^*$) during the modification process, leading to the proper stress redistribution within the flywheel domain.

To describe the behavior of a disk element of the flywheel, the following set of equilibrium equations has to be written:

$$\begin{aligned} \sigma_{r,r} + \tau_{,\varphi} / r + (\sigma_r - \sigma_t) / r + \mu r \omega^2 &= 0 \\ \sigma_{t,\varphi} / r + \tau_{,r} + 2\tau / r &= 0 \end{aligned} \quad (2)$$

accompanied by kinematical relations in the form:

$$\begin{aligned} \varepsilon_r &= u_{r,r} \\ \varepsilon_t &= u_{t,\varphi} / r + u_{r,r} \\ \gamma &= u_{t,r} - u_{t,r} + u_{r,\varphi} / r \end{aligned} \quad (3)$$

and linear strain-stress relations, following from the Hooke's law:

$$\begin{aligned}
\varepsilon_r &= (\sigma_r - \nu_d \sigma_t) / E_d \\
\varepsilon_t &= (\sigma_t - \nu_d \sigma_r) / E_d \\
\gamma &= \tau / G_d
\end{aligned} \tag{4}$$

The equations (2-4) are written in polar coordinate system (r, φ) (cf. Figure 2), and u_r, u_t denote the radial and circumferential displacement components, while $\varepsilon_r, \varepsilon_t, \gamma$ and σ_r, σ_t, τ are the strain and stress components, respectively.

The behavior of a discrete stiffening rib element can be described using similar equations as for the wheel domain. The ribs can be treated as curvilinear plane arches loaded along their middle line by distributed forces resulting from discontinuities of normal and tangential stresses within the disk domain on both sides of each rib, $\langle \sigma_{ns} \rangle, \langle \sigma_n \rangle$ (cf. Dems and Mróz 1992), see Figure 3.

Consequently, referring to Dems and Mróz 1987, one can write the following set of rib equilibrium equations:

$$\begin{aligned}
N_{,s} - M_{,s} K + \langle \sigma_{ns} \rangle &= 0 \\
NK + M_{,ss} + \langle \sigma_n \rangle &= 0
\end{aligned} \quad \text{along } \Gamma \tag{5}$$

where N, Q, M denote normal and tangential force as well as bending moment in rib cross-section, respectively. The subscript n and s denote here the normal and tangential components of a given quantity in the natural coordinate system. The symbol $\langle \cdot \rangle$ is used to describe the jump of the proper quantity and K is the curvature of the middle line of the rib. The kinematic relations for a rib element have the following form:

$$\varepsilon = u_{,s} - K u_n; \quad \theta = u_{,n} + K u_s; \quad \kappa = -\theta_{,s} \quad \text{along } \Gamma \tag{6}$$

where $\varepsilon, \kappa, \theta, \mathbf{u}(u_s, u_n)$ denote elongation, curvature, angle of cross section rotation and displacement of the rib element, respectively. The linear strain-stress relations for the rib element can be written in the form:

$$M = EI\kappa; \quad N = EA\varepsilon \quad \text{along } \Gamma \tag{7}$$

where EI and EA denote its bending and longitudinal rigidity. When the ribs can only transmit tensile forces, then their bending stiffness should tend to zero, and then the ribs can be treated as fibers in tension. Finally, the set of equations (1)-(7) has to be supplemented with continuity conditions of displacements along the middle lines of ribs, which can be written as follows:

$$\langle u_n \rangle = 0; \quad \langle u_s \rangle = 0 \quad \text{along } \Gamma \tag{8}$$

The above set of equations (1-4) and (5-7) describes the behavior of the flywheel with reinforcements of arbitrary shape starting and ending on its external and internal boundaries, respectively. It is obvious that service functionality of the proposed flywheel depends on the ability to store the kinematic energy, which is a simple function of mass distribution within the disk domain and its angular velocity. However, it is assumed that the mass redistribution is not considered here. Consequently, the only factor influencing energy density is angular velocity which has to be limited with respect to allowable damaged stress levels within disk and ribs domains. It can be stated that for the optimal flywheel the lowest possible local effective stresses are observed for an assumed level of angular velocity. This type of flywheel will be analyzed in the next Sections.

3. Problem formulation for composite flywheel

In this Section a different but commonly used approach for analysis of the reinforced flywheel structure is considered. When the number of fibers in the structure described earlier is relatively large, one will obtain a composite disk in which the role of reinforcements is played by fibers made of relatively strong material, continuously distributed within disk domain (cf. Figure 4). Such a flywheel can now be considered as a composite disk made of macroscopically homogeneous material, the mechanical properties of which can be obtained as the result of the homogenization procedure of its components. Hence, to describe the behavior of this type of flywheel, the set of equations similar to equations (2) and (3) has to be written and next supplemented with the strain-stress relation for homogenized orthotropic material, expressed in the form:

$$\boldsymbol{\sigma} = \begin{Bmatrix} \sigma_r \\ \sigma_t \\ \tau \end{Bmatrix} = \begin{bmatrix} D_{11} & D_{12} & D_{13} \\ D_{12} & D_{22} & D_{23} \\ D_{12} & D_{23} & D_{33} \end{bmatrix} \begin{Bmatrix} \varepsilon_r \\ \varepsilon_t \\ \gamma \end{Bmatrix} = \mathbf{D} \boldsymbol{\varepsilon} \quad (9)$$

where \mathbf{D} denotes the elasticity matrix written in the global polar coordinate system. Thus, the complete set of equations describing the problem at hand is composed from equations (2), (3) and (9). The matrix \mathbf{D} can be obtained using the transformation rule for elasticity matrix \mathbf{D}_0 , derived with respect to orthotropy axes at a given point of composite material (Figure 4). This transformation is written in the form:

$$\mathbf{D} = \mathbf{L}^T \mathbf{D}_0 \mathbf{L} \quad (10)$$

where \mathbf{L} is the transformation matrix from local to global coordinate systems, expressed as follows:

$$\mathbf{L} = \begin{bmatrix} \cos^2(\alpha) & \sin^2(\alpha) & -0.5\sin(2\alpha) \\ \sin^2(\alpha) & \cos^2(\alpha) & 0.5\sin(2\alpha) \\ \sin(2\alpha) & -\sin(2\alpha) & \cos(2\alpha) \end{bmatrix} \quad (11)$$

and α denotes the angle between the radial axis r and the line tangent to fiber at the given point. The elasticity matrix \mathbf{D}_0 for orthotropic material can be written as follows:

$$\mathbf{D}_0 = \begin{bmatrix} D_{11}^0 & D_{12}^0 & 0 \\ D_{12}^0 & D_{22}^0 & 0 \\ 0 & 0 & D_{33}^0 \end{bmatrix} \quad (12)$$

where its individual nonzero components D_{ij}^0 ($i, j=1, 2, 3$) are the functions of so called engineering constants of composite material, that is Young's moduli E_1 , E_2 in the orthotropy directions, shear modulus G and proper Poisson's ratios ν_{12} and ν_{21} . The nonzero components \mathbf{D}_0 are thus expressed in the form (Jones 1998):

$$\begin{aligned} D_{11} &= \frac{E_1}{1 - \nu_{12}\nu_{21}}, & D_{22} &= \frac{E_2}{1 - \nu_{12}\nu_{21}} \\ D_{33} &= G_{12}, & D_{12} &= \frac{\nu_{12}E_2}{1 - \nu_{12}\nu_{21}} = \frac{\nu_{21}E_1}{1 - \nu_{12}\nu_{21}} \end{aligned} \quad (13)$$

The above-mentioned engineering material parameters can be obtained using any homogenization approach. In this article, the Halpin-Tsai procedure (Jones 1998) will be adopted. According to this procedure, the engineering constants of composite material are expressed in the form:

$$\begin{aligned}
 E_1 &= E_f \rho_r + E_m (1 - \rho_r), & v_{12} &= v_f \rho + v_m (1 - \rho_r) \\
 E_2 &= E_m \frac{(1 + 2\eta \rho_r)}{(1 - \eta \rho_r)} & \text{where } \eta &= \frac{(E_f/E_m - 1)}{(E_f/E_m + 2)} \\
 G_{12} &= G_m \frac{(1 + \eta \rho_r)}{(1 - \eta \rho_r)} & \text{where } \eta &= \frac{(G_f/G_m - 1)}{(G_f/G_m + 1)} \\
 v_{21} &= v_{12} \frac{E_2}{E_1}
 \end{aligned} \tag{14}$$

where subscripts f and m distinguish the fiber and matrix properties, respectively, and ρ_r is variable density saturation of the composite matrix with the fibers material. It is assumed furthermore that fiber density varies along the radius of a flywheel similarly to the mass distribution of reinforcements in the disk discussed in the previous Section. Such assumption allows the comparison of these two approaches to the flywheel analysis within the class of disks with a prescribed volume of the reinforcing material.

The density ρ_r appearing in (14) can be evaluated using relations following from Figure 5. Assuming constant fiber thickness, its density at a given point of the disk can be expressed as:

$$\rho_r = w/m_n \tag{15}$$

where w denotes fiber thickness in the disk plane and m_n is a normal distance between two adjacent fibers. Taking into account the relation for average material density in the reinforced flywheel written in the form:

$$\rho = V_r/V_f \tag{16}$$

where V_r and V_f denote the reinforcement material volume and total flywheel volume, respectively, and using the relation following from Figure 5, the local varying fiber density can be expressed as follows:

$$\rho_r = \frac{\rho (r_e^2 - r_i^2)}{2lr \cos(\alpha)} \tag{17}$$

where l denotes the length of seach fiber line.

4. Optimal problem formulation

The main goal of the design process is to create the flywheel which can store as much kinetic energy as possible. To model the flywheel behavior, two models of the flywheel discussed in previous Sections will be used and subjected to a proper set of mechanical and other constraints. The optimal structure should satisfy the condition of the lowest local maximal effective stresses associated with the Huber-Misses yield condition. Then the global measure of local effective stresses within flywheel domain will be selected as the cost function in optimization procedure (see Kleiber *et al.* 1998).

4.1 Optimal problem formulation for rib-reinforced flywheel

Using the first approach for modeling the flywheel response, discussed in Section 2, it will be assumed that the shape of the middle line of each rib or fiber is the same and is described by the Bezier curve, which is

defined by the coordinates of the vertices of Bezier polygon. In the presented analysis, the shape of the Bezier curve is determined by four vertices defined in the local polar coordinate system (ξ, η) , as shown in Figure 6. Both coordinates of vertex "0" and radial coordinate of vertex "3" are fixed. Thus, the remaining coordinates of vertices of the Bezier polygon are chosen as design parameters and compose the vector of design variables $\mathbf{b} = \{ \xi_1, \eta_1, \xi_2, \eta_2, \xi_3 \}$.

The optimization problem for the rotating flywheel is now formulated in the following form:

$$\min G = \left[\frac{1}{A} \int \left(\frac{\sigma_{de}(\mathbf{b})}{\sigma_{d0}} \right)^k d\Omega \right]^{\frac{1}{k}} + \left[\frac{1}{l(\mathbf{b})} \int \left(\frac{\sigma_{fe}(\mathbf{b})}{\sigma_{f0}} \right)^k ds \right]^{\frac{1}{k}} \quad (18)$$

$$V(w(\mathbf{b}), l(\mathbf{b})) = V_0 = \text{const}$$

where σ_{de} and σ_{fe} denote the commonly used effective stresses within the disk and reinforcement domains, calculated according to Huber-Mises criterion (Mises R. V. 1913) while σ_{d0} and σ_{f0} are the assumed upper bounds of these stresses. The factor k is a natural even number and A denotes the flywheel area, while V is the volume function of reinforcing fibers and V_0 denotes its prescribed amount. Taking into account the assumption of constant fiber thickness, function V depends on w and l (see Figure 5). It should be noted that for k tending to infinity the functional G is a strict measure of maximal local effective stresses. The constraint applied in problem (18) can be treated as the upper bound imposed on the amount of reinforcing material. The question is how to redistribute this material for a given number of reinforcements in order to satisfy (18). The redistribution of this material is related to the length of the rib and its cross sectional area, as well as to the number of ribs introduced into disk domain. It was assumed that the cross-section of the reinforcement is a rectangle of a constant height, equal to flywheel thickness. Then the reinforcement width, varying during optimization process, is expressed as:

$$w = V_0 / (nh_0l) \quad (19)$$

where h_0 denotes height of the rib and n is the number of reinforcements.

Due to assumption (19), problem (18) can be treated as unconstrained, and defined as:

$$\min G_f = \left[\frac{1}{A} \int \left(\frac{\sigma_{de}}{\sigma_{d0}} \right)^k d\Omega \right]^{\frac{1}{k}} + \left[\frac{1}{l} \int \left(\frac{\sigma_{fe}}{\sigma_{f0}} \right)^k ds \right]^{\frac{1}{k}} \quad (20)$$

4.2 Optimal problem formulation for composite flywheel

Using now the second approach for modeling of the flywheel response, discussed already in Section 3, it is assumed that the line of each fiber is described similarly as in the previous case. Consequently, the design parameters are also defined in the same way.

Optimal problem formulation for a composite flywheel can be written in a form similar to (20), omitting its second part characteristic for explicit reinforcement. Thus, the optimal problem is formulated now as follows:

$$\min G_c = \left[\frac{1}{A} \int \left(\frac{\sigma_e(\mathbf{b})}{\sigma_0} \right)^k d\Omega \right]^{\frac{1}{k}} \quad (21)$$

where σ_e denote the effective stress within homogenized flywheel domain. The constraint imposed on constant fiber mass material, equivalent to constraint appearing in (18), is satisfied in view of the assumption associated with (17).

5. Optimization procedure

Looking for the global solution of optimization problems (20) or (21), a floating point genetic algorithm was used. This means that each chromosome in each population is explicitly related to design variables. A non-uniform Gaussian mutation, heuristic crossover and deterministic selection were chosen as the genetic operators. The termination of the algorithm was established by fitness convergence. The fitness function, being the measure of design quality, was assumed in the form:

$$f_i = e^{\left(-a \frac{(G_i - G_{\min})}{(G_{\max} - G_{\min})} \right)} \quad (22)$$

where G_i denotes the value of objective functional (20) or (21) associated with i th individual in current population, and G_{\max} and G_{\min} are the maximal and minimal values of (20) or (21) in this population. The definition of the fitness function guarantees its non-negativity and makes the difference of individual fitness more controllable which is an important factor for the selection stage. The positive factor a is used to control the probability of the individuals being selected to create a new population – the increasing value of a causes higher probability for selecting the individual with higher value of fitness function. The negative sign in front of a converts a minimization problem to the problem of maximization of fitness function.

The deterministic selection is performed under the assumption that the number of duplicates of a given individual (a set of variables describing one of the possible solutions) in the parent population is as close to the expected number as possible. The expected number of copies is described as a function of the size of population n and its fitness function f_i , and takes the form:

$$n_i = \frac{f_i}{\sum_{k=1}^n f_k} n \quad (23)$$

The heuristic crossover consists of extrapolation between two randomly chosen individuals (from the temporary population obtained after selection) which is performed in the direction of the individual possessing the greater fitness value. The maximum extrapolation amount is the difference between the two parent individuals. If the new individual does not fall into the variable bounds, a new extrapolation is performed. However, it is done no more times than the assumed number of attempts. If all attempts fail, the parent individuals are used as new children, otherwise the new individual and the previous individual having the greater fitness values are returned.

Finally, the non-uniform Gaussian mutation is performed during each cycle of the algorithm. It is the most advanced of the mutation operators. A new individual (after mutation) is chosen basing on a Gaussian distribution around the parent individual. The standard deviation of the Gaussian curve is chosen as a part of the variable range and decreases with increasing generation numbers. This is based on the assumption that the optimal individual is closer to the parent individual in the following generations. If the new value does not fall into the variable bounds, the process is repeated up to a maximum number of attempts. When all attempts fail, the original value is returned.

6. Numerical analysis of the flywheel behavior

The finite element method was used to calculate stress fields needed in functionals (20) or (21) for both approaches to flywheel analysis. Due to different physical models of the rib- or fiber-reinforced flywheel and the composite flywheel, various finite element approaches had to be chosen. The discretization of rib-reinforced disk was strongly influenced by the shape of the ribs and then had to be carried out along their middle lines (see Figure 7), while the composite disk was discretized using as regular a mesh as possible, with respect to the nonuniform macroscopic structure of the disk. In the discretization procedure, 8-nodal serendipity family elements were used for disk elements and 2-nodal bar elements in the case of pure tension of reinforcing fibers.

7. Optimal design results

To illustrate and compare two approaches to flywheel analysis, discussed in previous Sections, an illustrative example was considered and the influence of the varying number of reinforcements on the quality of the design was inspected. The results of the analysis are presented in this Section.

It was assumed that the component materials of a flywheel are isotropic and reinforcing fibers have the same material properties in both approaches used during analysis process. The disk of the flywheel was made from epoxy resin and the carbon fibers play the role of its reinforcements. The volume of reinforcement material was equal to 10% of the total structure volume. The external and internal radii r_e and r_i were set to 1000 and 200 [mm], respectively and the thickness of the flywheel was set to 20[mm]. The angular velocity was assumed to be equal to 1500 [r/min]. The upper bound of admissible stresses σ_{f0} appearing in (18) was assumed to be 30[MPa], while σ_{d0} was one hundred times smaller than σ_{f0} , and the factor k was set to 20.

The parameters of the evolutionary algorithm used in the optimization procedure were kept the same for both models of the flywheel. The number of individuals in each generation was constant and equal to 50. The probability of crossover and its maximal number of attempts (leading to create new admissible individual) were 1 and 5, respectively. The probability of mutation was 0.05 and maximal number of attempts was fixed to 5. The initial level of standard deviation of Gaussian mutation was 1/12 of the design variables range variability and was decreased 0.99 times per generation. The process of finding the best solution was terminated when the best individual during the last 10 generations was stable within 10^{-3} relative range. To avoid too strong finite element degeneration during the optimization process of the flywheel, the upper and lower bounds on design parameters, presented in Table 1, were assumed (see Figure 6):

The calculations for the rib-reinforced flywheel, using the approach presented in Section 2, were carried out for flywheels with 4, 8, 16, 32 and 48 discrete reinforcements carrying out only the tension force. This assumption was introduced in order to obtain a similar behavior of the structure as in the case of a flywheel reinforced with continuously distributed fibers. In the last case, the approach presented in Section 3 was applied to flywheel analysis.

The optimal shapes of reinforcements, obtained during optimization process using the first approach, are shown in Figure 8. It is easy to notice that the obtained shapes are close to straight lines in almost the whole domain of the flywheel, with exception to the domain in the neighborhood of the inner boundary. The angle ξ_1 (cf. Figure 6), describing the fiber shape in this domain, tends to its limit bounds (cf. Table 1) with the increasing number of fibers. Thus, in this domain, the fibers become tangential to the boundary as far as the bounds on ξ_1 allow it. Changes of optimal angle ξ_1 in function of number of ribs are shown in Figure 9.

In the case of the composite flywheel made of macroscopically homogeneous material (the second approach), the shape of reinforcing fibers does not influence the discretization process but influences only the elasticity matrix of the structure. Hence, the bounds of design variables could be much wider than in the

1
2
3 previous case, but still should be limited to avoid kinking of fibers - which is easy to satisfy assuming $\eta_2 > \eta_1$
4 (cf. Figure 6). In spite of it, the design parameters for the composite flywheel were subjected to the same
5 bounds as in the previous case, cf. Table 1. Such bounds were introduced here in order to compare both
6 approaches. The obtained optimal shape of fibers, using the approach presented in Section 3, is also depicted
7 in Figure 8. The angle of fiber middle line, near inner boundary of the disk, is equal to its bound $0.3[\text{rad}]$.
8 Moreover, the effective stresses in optimal flywheel were decreased about 40% in comparison with the
9 flywheel reinforced with straight fibers. The plots of effective stresses, in optimal and reference disks, are
10 shown in Figure 10a and 10b, respectively.
11

12
13 It is worthwhile to note that, using both approaches to analyze the flywheel behavior, one can observe that
14 the optimal shape of reinforcements in the neighborhood of inner boundary of a flywheel becomes tangential
15 to this boundary as far as the imposed bounds on design parameters allows on it. This type of behavior can be
16 explained by the influence of dominating circumferential stresses in this domain, influencing then the
17 effective stresses along inner boundary (see Figure 10 for the case of composite wheel). Moreover, the
18 obtained optimal rib-strengthening and composite flywheels present the optimal solution within the frame of
19 assumed models of a structure and strong design parameters bounds.
20

21 Using both analyzed approaches, the optimal reinforcements have similar shapes determined mainly by the
22 direction of fiber lines along the inner boundary. Similarity of these shapes in both approaches is closer with
23 the increasing number of discrete reinforcements within wheel domain. The similarity of optimal fiber shapes
24 using both approaches causes also the similar response behavior of flywheel, measured by the value of
25 functional (20) and (21). Comparing the optimal flywheel with 32 or 48 discrete ribs and the corresponding
26 optimal composite disk with the same volume of reinforcing material, one can observe that the differences
27 between the values of functional (20) and (21) are less than 1%. In other cases, for flywheels with smaller
28 number of reinforcements, these differences are about 5%.
29
30
31
32

33 8. Concluding remarks

34
35 Two approaches to analysis and optimal design of reinforced composite flywheels were discussed in this
36 article. When the number of reinforcements is relatively small, the approach basing on separate analysis of
37 behavior of the disk domain and reinforcements coupling through conditions of the continuity of displacement
38 field along reinforcement lines seems to be reasonable despite its complexity. On the other hand, with the
39 increasing number of reinforcements, the homogenization approach providing the homogeneous orthotropic
40 model of the rotating flywheel becomes more useful, mainly due its relative simplicity when compared with
41 the first approach.
42

43 As the results presented in the previous Section showed, the analysis for the composite flywheel, when
44 compared with the analysis for the flywheel with large number of discrete ribs, gives fairly good results and it
45 is much faster than for the discrete model of reinforcements. In other cases, when the number of
46 reinforcements is small, the time of calculation is similar using the two approaches, but the obtained optimal
47 flywheels are of different quality measured by proper objective functionals.
48

49 Only the case of the flywheel rotating with constant angular speed was considered in this article. However,
50 the analysis for the case of varying in time angular speed, influencing in obvious manner the optimal shape of
51 reinforcements, will follow the similar steps and will be presented in the consecutive article.
52
53
54
55

56 Acknowledgement

57 This work was supported by Grant No. 3955/T02/2007/32 of Ministry of Science and Higher Education
58
59
60

9. References

- Curtiss, D.H., Mongeau, P.P., Putrbaugh, R.L., 1995, Advanced composite flywheel structure design for a pulsed disk alternator, *IEEE Transactions on Magnetics*, 31, 26-31.
- Dems, K., Mróz, Z., 1987, A variational approach to sensitivity analysis and structural optimization of plane arches, *Mech. Struct. Mach.*, 15(3), 297-321
- Dems, K., Mroz, Z., 1992, Shape sensitivity analysis and optimal design of disks and plates with strong discontinuities of kinematic fields, *Int. J. Solids Struct.*, 29,4,437-463.
- Eby, D., et al., W., 1999, Optimal Design of Flywheels Using an Injection Island Genetic Algorithm, *Artificial Intelligence in Engineering Design, Analysis and Manufacturing*, 13, 389-402.
- Jones, R.M., 1998, *Mechanics Of Composite Materials*, Philadelphia: Taylor & Francis
- Kaftanoglu, B., Soylu, R., Oral, S., 1989, Mechanical energy storage using flywheels and design optimization. In: B. Kilic and S. Kakac, eds. *Energy Storage Systems*, Dordrecht: Kluwer Academic Publishers, 619-648.
- Kleiber, M. (Ed.), 1998, *Handbook of Computational Solid Mechanics*, Springer Verlag.
- Mises, R. V., 1913, *Mechanik de festen Körper im plastisch deformablem Zustand*, Götting. Nachr., Math. Phys. Kl., 582-592
- Ries, D.M., Kirk J.A., 1992, Design and manufacturing for a composite multi-ring flywheel, *27th Intersociety Energy Conversion Engineering Conference*, 4, 43-48.
- Thielman, S., Fabien, B.C., 2000, An optimal control approach to the design of stacked-ply composite flywheels, *Engineering Computations*, 17(5), 541-555.
- Turant, J., Dems, K., 2001, Sensitivity and optimal design of reinforcing interfaces in composite disks, *Fibers & Textiles in Eastern Europe*, January/March , 57 -62

Figure captions

Figure 1. Discrete (a) and continuously distributed (b) reinforcements in the flywheel.

Figure 2. Rib-reinforced flywheel.

Figure 3. Rib element subjected to the jumps of disk stresses.

Figure 4. Composite flywheel.

Figure 5. The schema of fiber distribution within disk domain.

Figure 6. Reinforcement line shape described by Bezier curve.

Figure 7. Discretization and decomposition of rib-reinforced flywheel using 8-nodal serendipity family disk elements and 2-nodal beam-bar elements.

Figure 8. Optimal shapes of reinforcements for both approaches.

Figure 9. Changes of angle ξ_1 versus number of ribs.

Figure 10. Effective stresses in the optimal (a) and reference (b) flywheels.

Table 1. Bounds on design parameters

	ξ_1 [rad]	η_1 [mm]	ξ_2 [rad]	η_2 [mm]	ξ_3 [rad]
lower bound	-0.3	200	-0.4	850	-0.6
upper bound	0.3	800	0.4	1000	0.6

For Peer Review Only

1
2
3
4
5
6
7
8
9
10
11
12
13
14
15
16
17
18
19
20
21
22
23
24
25
26
27
28
29
30
31
32
33
34
35
36
37
38
39
40
41
42
43
44
45
46
47
48
49
50
51
52
53
54
55
56
57
58
59
60

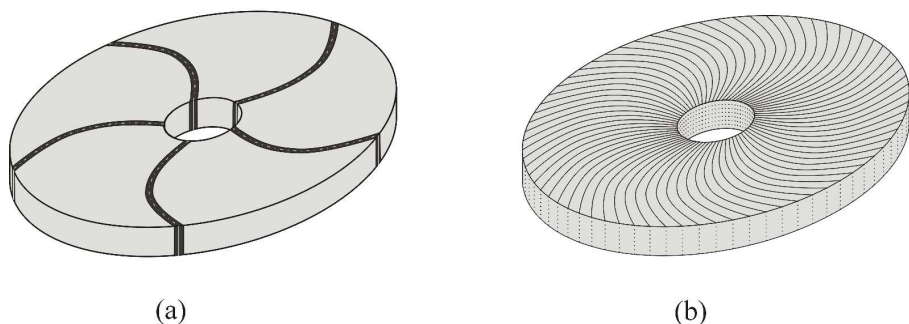


Figure 1 Discrete (a) and continuously distributed (b) reinforcements in the flywheel.

Peer Review Only

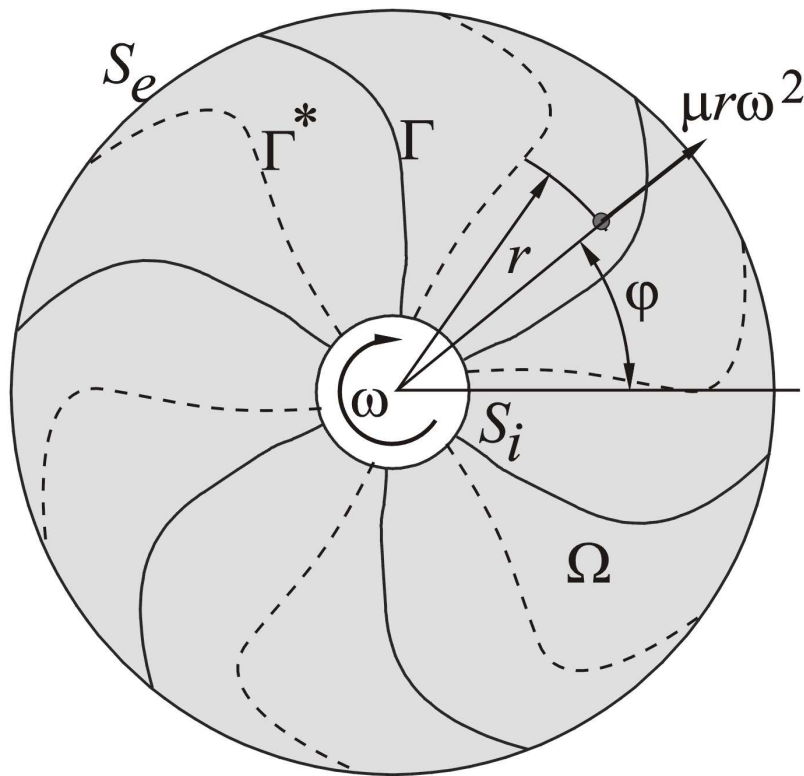


Figure 2. Rib-reinforced flywheel.

1
2
3
4
5
6
7
8
9
10
11
12
13
14
15
16
17
18
19
20
21
22
23
24
25
26
27
28
29
30
31
32
33
34
35
36
37
38
39
40
41
42
43
44
45
46
47
48
49
50
51
52
53
54
55
56
57
58
59
60

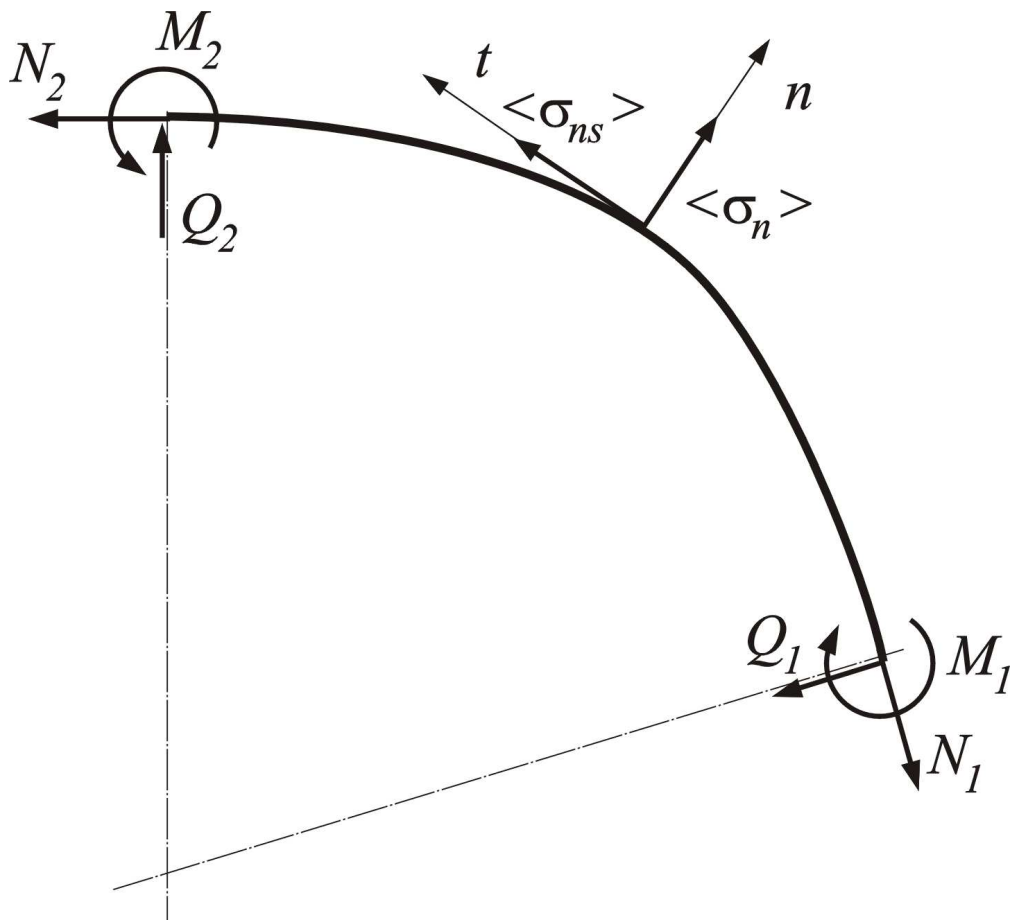


Figure 3. Rib element subjected to the jumps of disk stresses.

Only

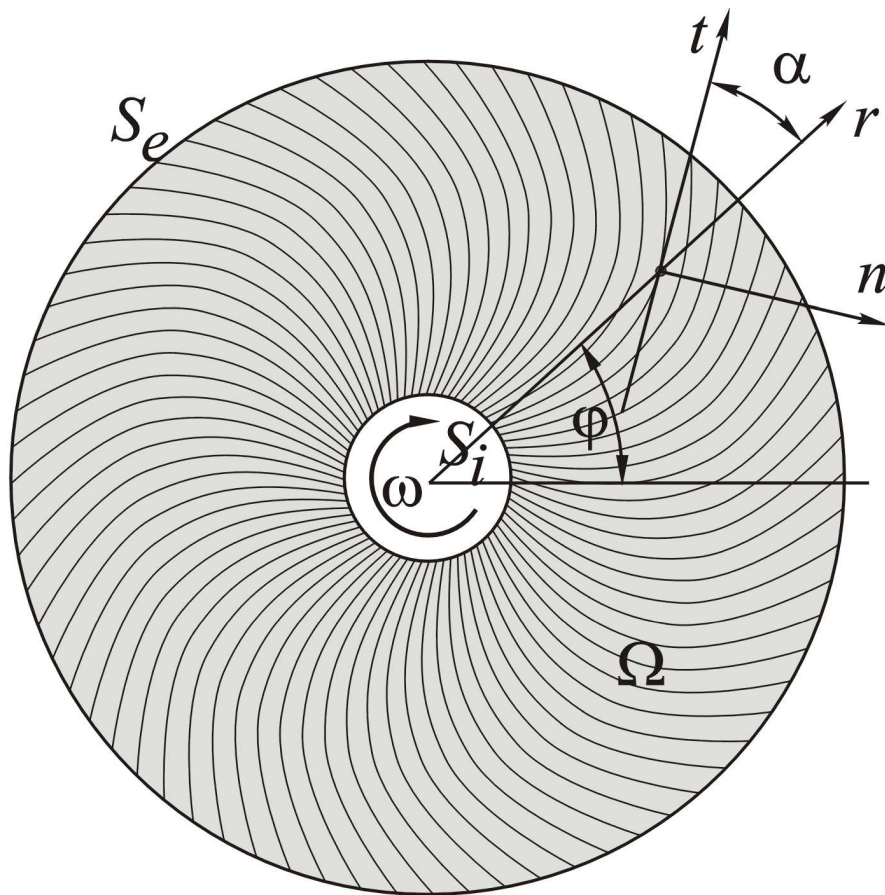


Figure 4. Composite flywheel.

Only

1
2
3
4
5
6
7
8
9
10
11
12
13
14
15
16
17
18
19
20
21
22
23
24
25
26
27
28
29
30
31
32
33
34
35
36
37
38
39
40
41
42
43
44
45
46
47
48
49
50
51
52
53
54
55
56
57
58
59
60

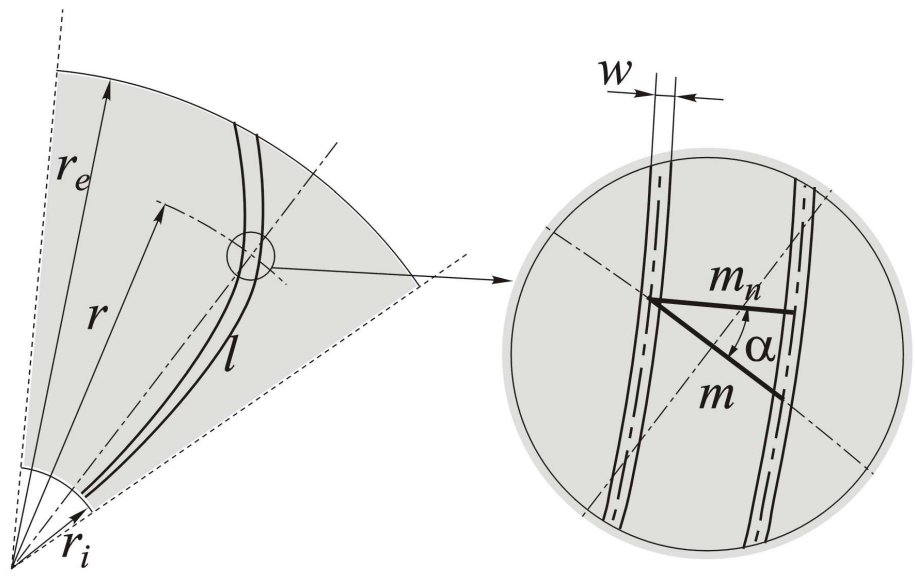


Figure 5. The schema of fiber distribution within disk domain.

Review Only

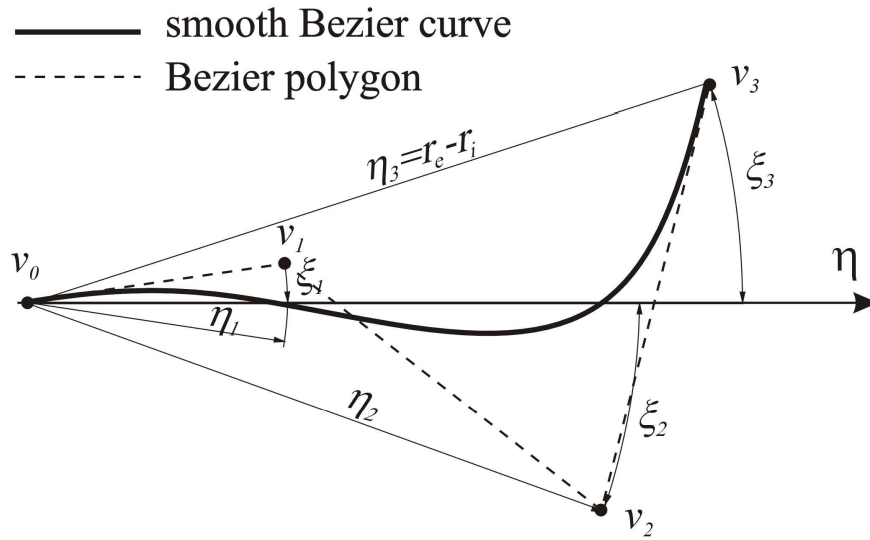


Figure 6. Reinforcement line shape described by Bezier curve.

Review Only

1
2
3
4
5
6
7
8
9
10
11
12
13
14
15
16
17
18
19
20
21
22
23
24
25
26
27
28
29
30
31
32
33
34
35
36
37
38
39
40
41
42
43
44
45
46
47
48
49
50
51
52
53
54
55
56
57
58
59
60

1
2
3
4
5
6
7
8
9
10
11
12
13
14
15
16
17
18
19
20
21
22
23
24
25
26
27
28
29
30
31
32
33
34
35
36
37
38
39
40
41
42
43
44
45
46
47
48
49
50
51
52
53
54
55
56
57
58
59
60

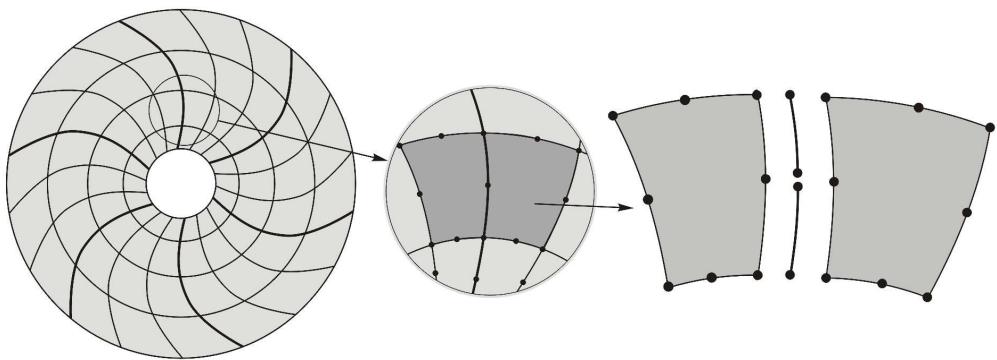


Figure 7. Discretization and decomposition of rib-reinforced flywheel using 8 nodal serendipity family disk elements and 2 nodal beam-bar elements.

Peer Review Only

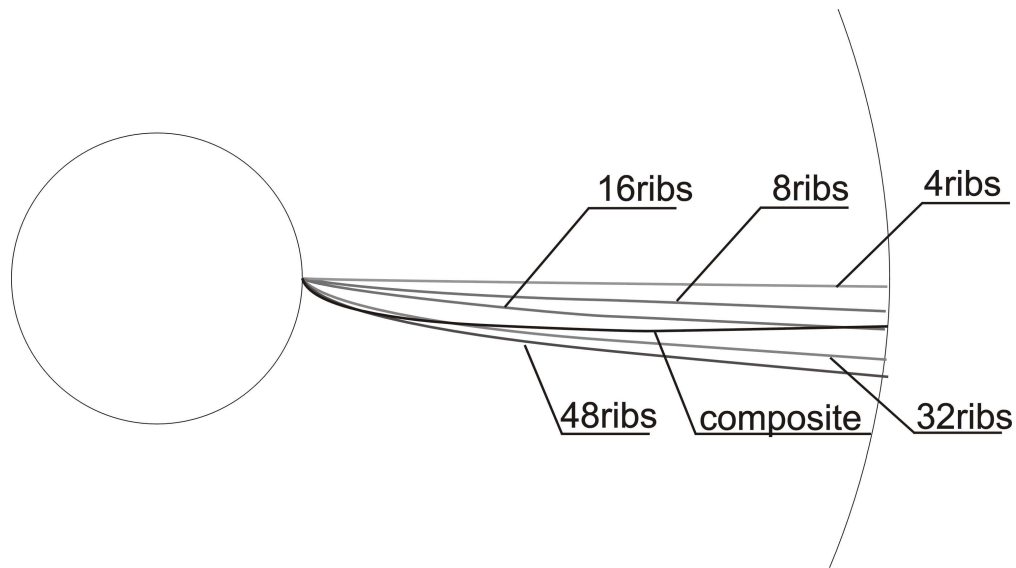


Figure 8. Optimal shapes of reinforcements for both approaches.

1
2
3
4
5
6
7
8
9
10
11
12
13
14
15
16
17
18
19
20
21
22
23
24
25
26
27
28
29
30
31
32
33
34
35
36
37
38
39
40
41
42
43
44
45
46
47
48
49
50
51
52
53
54
55
56
57
58
59
60

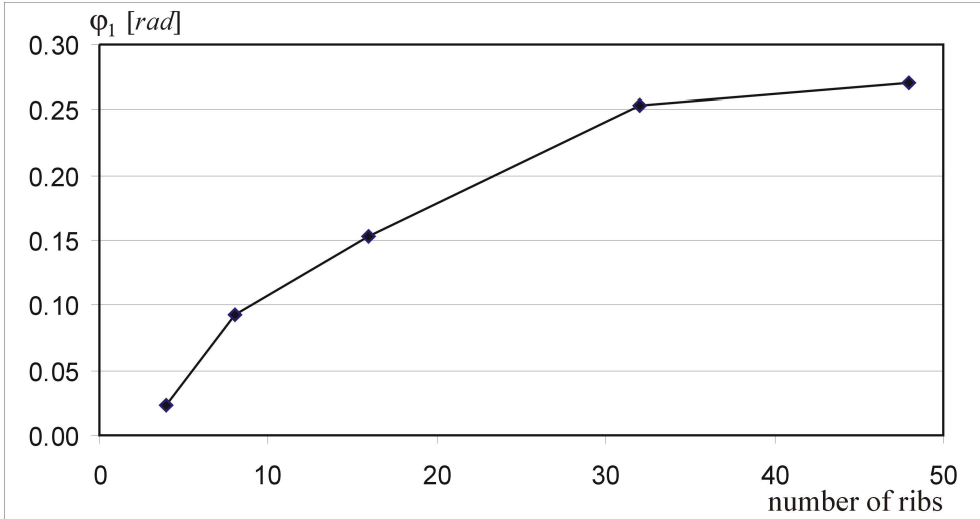


Figure 9. Changes of angle ϕ_1 versus number of ribs.

Review Only

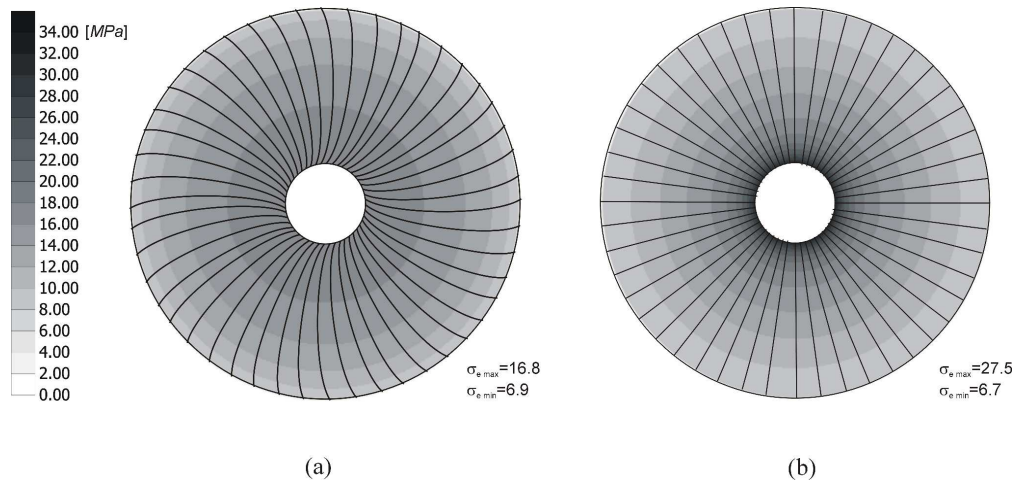


Figure 10. Effective stresses in the optimal (a) and reference (b) flywheels.

Two Approaches to Optimal Design of Composite Flywheel

Krzysztof Dems* and Jan Turant

Department of Technical Mechanics and Informatics, Technical University of Lodz, Lodz, Poland

In this paper two approaches to the design of reinforced composite flywheels are presented. The main goal of the optimization procedure is to maximize the accumulated kinetic energy of a flywheel. The first approach is based on a discrete model of reinforcement, causing the discontinuity of static fields along reinforcement and preserving the continuity of kinematic fields. In the second approach, the material of the reinforced flywheel is subjected to the homogenization procedure using the Halpin-Tsai assumption and then the continuity of both static and kinematic fields is preserved within flywheel domain. The evolutionary algorithm was used in both cases to determine the optimal shape of reinforcements, while the finite element method was applied in order to analyze the mechanical response of a flywheel.

Keywords: optimal design; composites; flywheels

1. Introduction

Flywheels are used in many devices when storing energy is needed. This type of the storage of energy has very important features making flywheels widely used. Flywheel kinetic energy is characterized by high cyclic lifetime, longtime reliability and its high level. These features are currently used in some vehicles for gathering energy lost during deceleration and in low earth orbit satellites which are unable to use their solar batteries while moving in the shadow of the earth. They can be also used in pulsed power supplies for electromagnetic guns or in **UPS (Uninterruptible Power Supply)** devices.

Due to their applicability there are many procedures solving this seemingly simple problem. Some designers concentrate their effort on proper redistribution of material properties and mass (Eby *et al.* 1999, Kaftanoglu *et al.* 1989, Ries and Kirk 1992) and others design variety of stack-ply composite structures (Curtiss *et al.* 1995, Thielman and Fabien 2000) to obtain flywheel with maximal energy density. These all approaches have one common feature: each of designed flywheels is made from durable light material, which is a natural consequence of the linear dependence of energy density with respect to mass density and quadratic dependence on angular velocity.

In this paper, design of fiber-reinforced flywheel of uniform thickness subjected to constant angular velocity is considered. The analysis of the case of the flywheel rotating with variable angular velocity will follow the similar steps and is not considered here.

Two different approaches to composite flywheel analysis are presented in the discussed design process. The first approach is based on the concept of reinforcing of the structure with a relatively small number of discrete ribs or fibers (cf. Figure 1a). In this case, the reinforcements introduced into flywheel domain cause the stress discontinuity and preserve continuity of displacement along the middle line of reinforcement (Dems and Mróz 1992, Turant and Dems 2001). The other approach assumes the continuous arrangement of a great number of reinforcements (cf. Figure 1b), which leads to the concept of material homogenization during analysis process (Jones 1998). In this model, the flywheel is treated as macroscopically uniform with its

* Email: krzysztof.dems@p.lodz.pl

material properties depending on material properties of fiber and matrix. Thus, two different models have to be considered for the purpose of disk analysis, taking into account the fundamental differences in two above mentioned approaches. It is assumed that the reinforcements introduced into the disk domain and disk itself are of the same thickness. Thus, the reinforcements constitute the integral part of the flywheel. The problem of delamination of the two phases within flywheel domain is not considered in this paper. Furthermore, the mass fraction and properties of material of reinforcements are the same in both approaches, and the materials of reinforcement and flywheel matrix are assumed to be elastically linear and isotropic. The shape of reinforcing fibers or ribs is described using smooth Bezier curve.

The energy accumulated in the flywheel depends on angular velocity, which also in obvious manner influences stress intensity. The stress distribution in fiber or rib reinforcing the wheel is a function of the orientation of the middle line of strengthening elements, and hence it can be changing during modification of reinforcement line shape. In the present paper, the main goal of designing process is to determine the shape of the reinforcing line so as to obtain the most strength flywheel. Such assumption leads to the design of the flywheel which can be subjected to maximal admissible angular velocity and consequently can store the maximal kinematic energy. Both approaches, i.e. discretely and continuously distributed reinforcements, are discussed and the results of design procedure are compared.

2. Problem formulation for flywheel with discrete rib-reinforcement

The composite flywheel of uniform thickness (cf. Figure 2), rotating with constant angular velocity ω and then loaded by distributed centrifugal force equal to $\mu r \omega^2$, is considered. μ denotes here an average matrix and fiber mass density and r determines the radial coordinate of a chosen material point. The flywheel has free external boundary S_e and it is supported on the internal boundary S_i so that the tangential displacements are equal to zero.

$$u_t = 0 \quad \text{along } S_i \quad (1)$$

The flywheel is composed from the uniform disk reinforced with some fibers or ribs introduced in its domain, whose number is relatively small. The volume of reinforcements is assumed to be constant but the shape of their middle lines can undergo changes ($\Gamma \rightarrow \Gamma^*$) during the modification process, leading to the proper stress redistribution within flywheel domain.

To describe the behavior of a disk element of the flywheel, the following set of equilibrium equations has to be written:

$$\begin{aligned} \sigma_{r,r} + \tau_{,\varphi} / r + (\sigma_r - \sigma_t) / r + \mu r \omega^2 &= 0 \\ \sigma_{t,\varphi} / r + \tau_{,r} + 2\tau / r &= 0 \end{aligned} \quad (2)$$

accompanied by kinematical relations in the form:

$$\begin{aligned} \varepsilon_r &= u_{r,r} \\ \varepsilon_t &= u_{t,\varphi} / r + u_{r,r} \\ \gamma &= u_{t,r} - u_{t,r} + u_{r,\varphi} / r \end{aligned} \quad (3)$$

and linear strain-stress relations, following from the Hooke's law:

$$\begin{aligned}\varepsilon_r &= (\sigma_r - \nu_d \sigma_t) / E_d \\ \varepsilon_t &= (\sigma_t - \nu_d \sigma_r) / E_d \\ \gamma &= \tau / G_d\end{aligned}\quad (4)$$

The equations (2-4) are written in polar coordinate system (r, φ) (cf. Figure 2), and u_r, u_t denote the radial and circumferential displacement components, while $\varepsilon_r, \varepsilon_t, \gamma$ and σ_r, σ_t, τ are the strain and stress components, respectively.

The behavior of discrete stiffening rib element can be described using the similar type of equations as for the wheel domain. The ribs can be treated as curvilinear plane arches loaded along their middle line by distributed forces resulting from discontinuities of normal and tangential stresses within disk domain on both sides of each rib, $\langle \sigma_{ns} \rangle, \langle \sigma_n \rangle$ (cf. Dems and Mróz 1992), see Figure 3.

Consequently, referring to Dems and Mróz 1987, one can write the following set of rib equilibrium equations:

$$\begin{aligned}N_{,s} - M_{,s} K + \langle \sigma_{ns} \rangle &= 0 \\ NK + M_{,ss} + \langle \sigma_n \rangle &= 0\end{aligned}\quad \text{along } \Gamma \quad (5)$$

where N, Q, M denote normal and tangential force as well as bending moment in rib cross-section, respectively. The subscript n and s denote here the normal and tangential components of a given quantity in the natural coordinate system. The symbol $\langle \cdot \rangle$ is used to describe the jump of the proper quantity and K is the curvature of the middle line of the rib. The kinematic relations for a rib element have the following form:

$$\varepsilon = u_{,s} - K u_n; \quad \theta = u_{,n} + K u_s; \quad \kappa = -\theta_{,s} \quad \text{along } \Gamma \quad (6)$$

where $\varepsilon, \kappa, \theta, \mathbf{u}(u_s, u_n)$ denote elongation, curvature, angle of cross section rotation and displacement of the rib element, respectively. The linear strain-stress relations for the rib element can be written in the form:

$$M = EI\kappa; \quad N = EA\varepsilon \quad \text{along } \Gamma \quad (7)$$

where EI and EA denote its bending and longitudinal rigidity. When the ribs can only transmit the tension forces, then their bending stiffness should tend to zero, and then the ribs can be treated as fibers in tension. Finally, the set of equations (1)-(7) has to be supplemented with continuity conditions of displacements along the middle lines of ribs, which can be written as follows:

$$\langle u_n \rangle = 0; \quad \langle u_s \rangle = 0 \quad \text{along } \Gamma \quad (8)$$

The above set of equations (1-4) and (5-7) describes the behavior of the flywheel with reinforcements of arbitrary shape starting and ending on its external and internal boundaries, respectively. It is obvious that service functionality of the proposed flywheel depends on the ability to store the kinematic energy, which is the simple function of mass distribution within disk domain and its angular velocity. However, it is assumed that the mass redistribution is not considered here. Consequently, the only factor influencing energy density is angular velocity which has to be limited with respect to allowable damaged stress level within disk and ribs domains. It can be stated that for the optimal flywheel the possibly lowest local effective stresses are observed for assumed level of angular velocity. Such type of the flywheel will be analyzed in the next Sections.

3. Problem formulation for composite flywheel

In this Section a different but commonly used approach for analysis of the reinforced flywheel structure is considered. When the number of fibers in the structure described earlier is relatively large, one will obtain composite disk in which the role of reinforcements play fibers made of relatively strong material, continuously distributed within disk domain (cf. Figure 4). Such flywheel can now be considered as composite disk made of macroscopically homogeneous material, which mechanical properties can be obtained as the result of the homogenization procedure of its components. Hence, to describe the behavior of this type of flywheel, the set of equations similar to equations (2) and (3) has to be written and next supplemented with the strain-stress relation for homogenized orthotropic material, expressed in the form:

$$\boldsymbol{\sigma} = \begin{Bmatrix} \sigma_r \\ \sigma_t \\ \tau \end{Bmatrix} = \begin{bmatrix} D_{11} & D_{12} & D_{13} \\ D_{12} & D_{22} & D_{23} \\ D_{12} & D_{23} & D_{33} \end{bmatrix} \begin{Bmatrix} \varepsilon_r \\ \varepsilon_t \\ \gamma \end{Bmatrix} = \mathbf{D} \boldsymbol{\varepsilon} \quad (9)$$

where \mathbf{D} denotes the elasticity matrix written in the global polar coordinate system. Thus, the complete set of equations describing the problem at hand is composed from equations (2), (3) and (9). The matrix \mathbf{D} can be obtained using the transformation rule for elasticity matrix \mathbf{D}_o , derived with respect to orthotropy axes at a given point of composite material (Figure 4). This transformation is written in the form:

$$\mathbf{D} = \mathbf{L}^T \mathbf{D}_o \mathbf{L} \quad (10)$$

where \mathbf{L} is the transformation matrix from local to global coordinate systems, expressed as follows:

$$\mathbf{L} = \begin{bmatrix} \cos^2(\alpha) & \sin^2(\alpha) & -0.5\sin(2\alpha) \\ \sin^2(\alpha) & \cos^2(\alpha) & 0.5\sin(2\alpha) \\ \sin(2\alpha) & -\sin(2\alpha) & \cos(2\alpha) \end{bmatrix} \quad (11)$$

and α denotes the angle between the radial axis r and the line tangent to fiber at the given point. The elasticity matrix \mathbf{D}_o for orthotropic material can be written as follows:

$$\mathbf{D}_o = \begin{bmatrix} D_{11}^0 & D_{12}^0 & 0 \\ D_{12}^0 & D_{22}^0 & 0 \\ 0 & 0 & D_{33}^0 \end{bmatrix} \quad (12)$$

where its individual nonzero components D_{ij}^0 ($i, j=1,2,3$) are the functions of so called engineering constants of composite material, that is Young's moduli E_1 , E_2 in the orthotropy directions, shear modulus G and proper Poisson's ratios ν_{12} and ν_{21} . The nonzero components \mathbf{D}_o are thus expressed in the form (Jones 1998):

$$\begin{aligned} D_{11} &= \frac{E_1}{1 - \nu_{12}\nu_{21}}, & D_{22} &= \frac{E_2}{1 - \nu_{12}\nu_{21}} \\ D_{33} &= G_{12}, & D_{12} &= \frac{\nu_{12}E_2}{1 - \nu_{12}\nu_{21}} = \frac{\nu_{21}E_1}{1 - \nu_{12}\nu_{21}} \end{aligned} \quad (13)$$

The above mentioned engineering material parameters can be obtained using any homogenization approach. In this paper, the Halpin-Tsai procedure (Jones 1998) will be adopted. According to this procedure, the engineering constants of composite material are expressed in the form:

$$\begin{aligned}
 E_1 &= E_f \rho_r + E_m (1 - \rho_r), & \nu_{12} &= \nu_f \rho + \nu_m (1 - \rho_r) \\
 E_2 &= E_m \frac{(1 + 2\eta \rho_r)}{(1 - \eta \rho_r)} & \text{where } \eta &= \frac{(E_f/E_m - 1)}{(E_f/E_m + 2)} \\
 G_{12} &= G_m \frac{(1 + \eta \rho_r)}{(1 - \eta \rho_r)} & \text{where } \eta &= \frac{(G_f/G_m - 1)}{(G_f/G_m + 1)} \\
 \nu_{21} &= \nu_{12} \frac{E_2}{E_1}
 \end{aligned} \tag{14}$$

where subscripts f and m distinguish the fiber and matrix properties, respectively, and ρ_r is variable density saturation of the composite matrix with the fibers material. It is assumed furthermore that fiber density varies along radius of a flywheel similarly as the mass distribution of reinforcements in the disk discussed in the previous Section. Such assumption allows to compare these two approaches to the flywheel analysis within the class of disks with the prescribed volume of the reinforcing material.

The density ρ_r appearing in (14) can be evaluated using relations following from Figure 5. Assuming constant fiber thickness, its density at a given point of the disk can be expressed as:

$$\rho_r = w/m_n \tag{15}$$

where w denotes fiber thickness in the disk plane and m_n is a normal distance between two adjacent fibers. Taking into account the relation for average material density in the reinforced flywheel written in the form:

$$\rho = V_r/V_f \tag{16}$$

where V_r and V_f denote the reinforcement material volume and total flywheel volume, respectively, and using the relation following from Figure 5, the local varying fiber density can be expressed as follows:

$$\rho_r = \frac{\rho (r_e^2 - r_i^2)}{2lr \cos(\alpha)} \tag{17}$$

where l denotes the length of seach fiber line.

4. Optimal problem formulation

The main goal of the design process is to create the flywheel which could store as much kinetic energy as possible. To model the flywheel behavior, two models of the flywheel discussed in previous Sections will be used and subjected to a proper set of mechanical and other constraints. The optimal structure should satisfy the condition of the lowest local maximal effective stresses associated with the Huber-Misses yield condition. Then the global measure of local effective stresses within flywheel domain will be selected as the cost function in optimization procedure (see Kleiber *et al.* 1998).

4.1 Optimal problem formulation for rib-reinforced flywheel

Using the first approach for modeling the flywheel response, discussed in Section 2, it will be assumed that the shape of the middle line of each rib or fiber is the same and it is described by the Bezier curve, which is

defined by the coordinates of the vertices of Bezier polygon. In the presented analysis, the shape of Bezier curve is determined by four vertices defined in the local polar coordinate system (ξ, η) , as it is shown in Figure 6. Both coordinates of vertex "0" and radial coordinate of vertex "3" are fixed. Thus, the remaining coordinates of vertices of Bezier polygon are chosen as design parameters and compose the vector of design variables $\mathbf{b} = \{\xi_1, \eta_1, \xi_2, \eta_2, \xi_3\}$.

The optimization problem for the rotating flywheel is now formulated in the following form:

$$\min G = \left[\frac{1}{A} \int \left(\frac{\sigma_{de}(\mathbf{b})}{\sigma_{d0}} \right)^k d\Omega \right]^{\frac{1}{k}} + \left[\frac{1}{l(\mathbf{b})} \int \left(\frac{\sigma_{fe}(\mathbf{b})}{\sigma_{f0}} \right)^k ds \right]^{\frac{1}{k}} \quad (18)$$

$$V(w(\mathbf{b}), l(\mathbf{b})) = V_0 = \text{const}$$

where σ_{de} and σ_{fe} denote the commonly used effective stresses within the disk and reinforcement domains, calculated according to Huber-Mises criterion (Mises R. V. 1913) while σ_{d0} and σ_{f0} are the assumed upper bounds of these stresses. The factor k is a natural even number and A denotes the flywheel area, while V is the volume function of reinforcing fibers and V_0 denotes its prescribed amount. Taking into account the assumption of constant fiber thickness, function V depends on w and l (see Figure 5). It should be noted that for k tending to infinity the functional G is a strict measure of maximal local effective stresses. The constraint applied in problem (18) can be treated as the upper bound imposed on the amount of reinforcing material. The question is how to redistribute this material for a given number of reinforcements in order to satisfy (18). The redistribution of this material is related to the length of the rib and its cross sectional area, as well as to the number of ribs introduced into disk domain. It was assumed that the cross-section of the reinforcement is a rectangle of a constant height, equal to flywheel thickness. Then the reinforcement width, varying during optimization process, is expressed as:

$$w = V_0 / (nh_0l) \quad (19)$$

where h_0 denotes height of the rib and n is the number of reinforcements.

Due to assumption (19), problem (18) can be treated as unconstrained, and defined as:

$$\min G_f = \left[\frac{1}{A} \int \left(\frac{\sigma_{de}}{\sigma_{d0}} \right)^k d\Omega \right]^{\frac{1}{k}} + \left[\frac{1}{l} \int \left(\frac{\sigma_{fe}}{\sigma_{f0}} \right)^k ds \right]^{\frac{1}{k}} \quad (20)$$

4.2 Optimal problem formulation for composite flywheel

Using now the second approach for modeling of the flywheel response, discussed already in Section 3, it is assumed that the line of each fiber is described similarly as in the previous case. Consequently, the design parameters are also defined in the same way.

Optimal problem formulation for a composite flywheel can be written in the form similar to (20), omitting its second part characteristic for explicit reinforcement. Thus, the optimal problem is formulated now as follows:

$$\min G_c = \left[\frac{1}{A} \int \left(\frac{\sigma_e(\mathbf{b})}{\sigma_0} \right)^k d\Omega \right]^{\frac{1}{k}} \quad (21)$$

where σ_e denote the effective stress within homogenized flywheel domain. The constraint imposed on constant fiber mass material, equivalent to constraint appearing in (18), is satisfied in view of the assumption associated with (17).

5. Optimization procedure

Looking for the global solution of optimization problems (20) or (21), a floating point genetic algorithm was used. That means that each chromosome in each population is explicitly related to design variables. A non-uniform Gaussian mutation, heuristic crossover and deterministic selection were chosen as the genetic operators. The termination of the algorithm was established by fitness convergence. The fitness function, being the measure of design quality, was assumed in the form:

$$f_i = e^{\left(-a \frac{(G_i - G_{\min})}{(G_{\max} - G_{\min})} \right)} \quad (22)$$

where G_i denotes the value of objective functional (20) or (21) associated with i -th individual in current population, and G_{\max} and G_{\min} are the maximal and minimal values of (20) or (21) in this population. The definition of the fitness function guarantees its non-negativity and makes the difference of individual fitness more controllable which is an important factor for the selection stage. The positive factor a is used to control the probability of the individuals being selected to create a new population – the increasing value of a causes higher probability for selecting the individual with higher value of fitness function. The negative sign in front of a converts a minimum problem to problem of maximization of fitness function.

The deterministic selection is performed under the assumption that the number of duplicates of a given individual (a set of variables describing one of the possible solutions) in parent population is as close to the expected number as possible. The expected number of copies is described as a function of the size of population n and its fitness function f_i , and takes the form:

$$n_i = \frac{f_i}{\sum_{k=1}^n f_k} n \quad (23)$$

The heuristic crossover consists of extrapolation between two randomly chosen individuals (from the temporary population obtained after selection) which is performed in the direction of the individual possessing the greater fitness value. The maximum extrapolation amount is the difference between the two parent individuals. If the new individual does not fall into the variable bounds, a new extrapolation is performed. However, it is done no more times than the assumed number of attempts. If all attempts fail, the parent individuals are used as new children, otherwise the new individual and the previous individual having the greater fitness values are returned.

Finally, the non-uniform Gaussian mutation is performed during each cycle of the algorithm. It is the most advanced of the mutation operators. A new individual (after mutation) is chosen basing on a Gaussian distribution around the parent individual. The standard deviation of the Gaussian curve is chosen as a part of the variable range and decreases with increasing generation numbers. This is based on the assumption that the optimal individual is closer to the parent individual in the following generations. If the new value does not fall into the variable bounds, the process is repeated up to a maximum number of attempts. When all attempts fail, the original value is returned.

6. Numerical analysis of the flywheel behavior

The finite element method was used to calculate stress fields needed in functionals (20) or (21) for both approaches to flywheel analysis. Due to different physical models of the rib- or fiber-reinforced flywheel and the composite flywheel, various finite element approaches had to be chosen. The discretization of rib-reinforced disk was strongly influenced by the shape of the ribs and then had to be carried out along their middle lines (see Figure 7), while the composite disk was discretized using as regular mesh as possible, with respect to uniform macroscopic structure of the disk. In the discretization procedure, 8-nodal serendipity family elements were used for disk elements and 2-nodal bar elements in the case of pure tension of reinforcing fibers.

7. Optimal design results

To illustrate and compare two approaches to flywheel analysis, discussed in previous Sections, an illustrative example was considered and the influence of the varying number of reinforcements on the quality of the design was inspected. The results of analysis are presented in this Section.

It was assumed that the component materials of a flywheel are isotropic and reinforcing fibers have the same material properties in both approaches used during analysis process. The disk of the flywheel was made from epoxy resin and the carbon fibers play the role of its reinforcements. The volume of reinforcement material was equal to 10% of the total structure volume. The external and internal radii r_e and r_i were set to 1000 and 200 [mm], respectively and the thickness of the flywheel was set to 20[mm]. The angular velocity was assumed to be equal to 1500 [r/min]. The upper bound of admissible stresses σ_{f0} appearing in (18) was assumed to be 30[MPa], while σ_{d0} was one hundred times smaller than σ_{f0} , and the factor k was set to 20.

The parameters of evolutionary algorithm used in optimization procedure were kept the same for both models of the flywheel. The number of individuals in each generation was constant and equal to 50. The probability of crossover and its maximal number of attempts (leading to create new admissible individual) were 1 and 5, respectively. The probability of mutation was 0.05 and maximal number of attempts was fixed to 5. The initial level of standard deviation of Gaussian mutation was 1/12 of the design variables range variability and was decreased 0.99 times per generation. The process of finding the best solution was terminated when the best individual during the last 10 generations was stable within 10^{-3} relative range. To avoid too strong finite element degeneration during the optimization process of the flywheel, the upper and lower bounds on design parameters, presented in Table 1, were assumed (see Figure 6):

The calculations for the rib-reinforced flywheel, using approach presented in Section 2, were carried out for flywheels with 4, 8, 16, 32 and 48 discrete reinforcements carrying out only the tension force. Such assumption was introduced in order to obtain a similar behavior of the structure as in the case of a flywheel reinforced with continuously distributed fibers. In the last case, the approach presented in Section 3 was applied to flywheel analysis.

The optimal shapes of reinforcements, obtained during optimization process using the first approach, are shown in Figure 8. It is easy to notice that the obtained shapes are close to straight lines in almost the whole domain of the flywheel, with exception to the domain in the neighborhood of the inner boundary. The angle ξ_1 (cf. Figure 6), describing the fiber shape in this domain, tends to its limit bounds (cf. Table 1) with the increasing number of fibers. Thus, in this domain, the fibers become tangential to the boundary as far as the bounds on ξ_1 allow it. Changes of optimal angle ξ_1 in function of number of ribs are shown in Figure 9.

In the case of the composite flywheel made of macroscopically homogeneous material (the second approach), the shape of reinforcing fibers does not influence discretization process but influences only the elasticity matrix of the structure. Hence, the bounds of design variables could be much wider than in the

1
2
3 previous case, but still should be limited to avoid kinking of fibers - which is easy to satisfy assuming $\eta_2 > \eta_1$
4 (cf. Figure 6). In spite of it, the design parameters for the composite flywheel were subjected to the same
5 bounds as in the previous case, cf. Table 1. Such bounds were introduced here in order to compare both
6 approaches. The obtained optimal shape of fibers, using the approach presented in Section 3, is also depicted
7 in Figure 8. The angle of fiber middle line, near inner boundary of the disk, is equal to its bound $0.3[\text{rad}]$.
8 Moreover, the effective stresses in optimal flywheel were decreased about 40% in comparison with the
9 flywheel reinforced with straight fibers. The plots of effective stresses, in optimal and reference disks, are
10 shown in Figure 10a and 10b, respectively.
11
12

13 It is worth to notice, that using both approaches to analyze the flywheel behavior, one can observe that the
14 optimal shape of reinforcements in the neighborhood of inner boundary of a flywheel becomes tangential to
15 this boundary as far as the imposed bounds on design parameters allows on it. This type of behavior can be
16 explained by the influence of dominating circumferential stresses in this domain, influencing then the
17 effective stresses along inner boundary (see Figure 10 for the case of composite wheel). Moreover, the
18 obtained optimal rib-strengthening and composite flywheels present the optimal solution within the frame of
19 assumed models of a structure and strong design parameters bounds.
20

21 Using both analyzed approaches, the optimal reinforcements have the similar shape determined mainly by
22 the direction of fiber lines along inner boundary. Similarity of these shapes in both approaches is closer with
23 the increasing number of discrete reinforcements within wheel domain. The similarity of optimal fiber shapes
24 using both approaches causes also the similar response behavior of flywheel, measured by the value of
25 functional (20) and (21). Comparing the optimal flywheel with 32 or 48 discrete ribs and corresponding
26 optimal composite disk with the same volume of reinforcing material, one can observe that the differences
27 between the values of functional (20) and (21) are less than 1%. In other cases, for flywheels with smaller
28 number of reinforcements, these differences are about 5%.
29
30
31
32

33 8. Concluding remarks

34
35 The two approaches to analysis and optimal design of reinforced composite flywheel were discussed in this
36 paper. When the number of reinforcements is relatively small, the approach basing on separate analysis of
37 behavior of the disk domain and reinforcements coupling through conditions of the continuity of displacement
38 field along reinforcement lines seems to be reasonable despite its complexity. On the other hand, with the
39 increasing number of reinforcements, the homogenization approach providing the homogeneous orthotropic
40 model of the rotating flywheel becomes more useful, mainly due its relative simplicity when compared with
41 the first approach.
42

43 As it come out from the results presented in the previous Section, the analysis for the composite flywheel,
44 when compared with the analysis for the flywheel with large number of discrete ribs, give fairly good results
45 and it is much faster than for the discrete model of reinforcements. In other cases, when the number of
46 reinforcements is small, the time of calculation is similar using approaches, but the obtained optimal
47 flywheels are of different quality measured by proper objective functionals.
48

49 Only the case of the flywheel rotating with constant angular speed was considered in this paper. However,
50 the analysis for the case of varying in time angular speed, influencing in obvious manner the optimal shape of
51 reinforcements, will follow the similar steps and will be presented in the consecutive paper.
52
53
54
55

56 Acknowledgement

57 This work was supported by Grant No. 3955/T02/2007/32 of Ministry of Science and Higher Education
58
59
60

9. References

- Curtiss, D.H., Mongeau, P.P., Putrbaugh, R.L., 1995, Advanced composite flywheel structure design for a pulsed disk alternator, *IEEE Transactions on Magnetics*, 31, 26-31.
- Dems, K., Mróz, Z., 1987, A variational approach to sensitivity analysis and structural optimization of plane arches, *Mech. Struct. Mach.*, 15(3), 297-321
- Dems, K., Mroz, Z., 1992, Shape sensitivity analysis and optimal design of disks and plates with strong discontinuities of kinematic fields, *Int. J. Solids Struct.*, 29,4,437-463.
- Eby, D., et al., W., 1999, Optimal Design of Flywheels Using an Injection Island Genetic Algorithm, *Artificial Intelligence in Engineering Design, Analysis and Manufacturing*, 13, 389-402.
- Jones, R.M., 1998, *Mechanics Of Composite Materials*, Philadelphia: Taylor & Francis
- Kaftanoglu, B., Soylu, R., Oral, S., 1989, Mechanical energy storage using flywheels and design optimization. In: B. Kilic and S. Kakac, eds. *Energy Storage Systems*, Dordrecht: Kluwer Academic Publishers, 619-648.
- Kleiber, M. (Ed.), 1998, *Handbook of Computational Solid Mechanics*, Springer Verlag.
- Mises, R. V., 1913, *Mechanik de festen Körper im plastisch deformablem Zustand*, Götting. Nachr., Math. Phys. Kl., 582-592
- Ries, D.M., Kirk J.A., 1992, Design and manufacturing for a composite multi-ring flywheel, *27th Intersociety Energy Conversion Engineering Conference*, 4, 43-48.
- Thielman, S., Fabien, B.C., 2000, An optimal control approach to the design of stacked-ply composite flywheels, *Engineering Computations*, 17(5), 541-555.
- Turant, J., Dems, K., 2001, Sensitivity and optimal design of reinforcing interfaces in composite disks, *Fibers & Textiles in Eastern Europe*, January/March , 57 -62